Generative Flows as a General Purpose Solution for Inverse Problems

José A. Chávez jose.chavez.alvarez@ucsp.edu.pe

Abstract

Due to the success of generative flows to model data distributions, they have been explored in inverse problems. Given a pre-trained generative flow, previous work proposed to minimize the 2-norm of the latent variables as a regularization term in the main objective. The intuition behind it was to ensure high likelihood latent variables, however this does not ensure the generation of realistic samples as we show in our experiments. We therefore propose a regularization term to directly produce high likelihood reconstructions. Our hypothesis is that our method could make generative flows a general-purpose solver for inverse problems. We evaluate our method in image denoising, image deblurring, image inpainting, and image colorization. We observe a compelling improvement of our method over prior works in the PSNR and SSIM metrics.

1 Introduction

With the success of generative models in the generation of synthetic data [10, 8], prior works [3, 1, 2] explored generative models for inverse problems in image processing. In an inverse problem we aim to recover $x^* \in \mathbb{R}^n$ from the possible-noisy linear measurements $y = Ax^* + \eta$, where $A \in \mathbb{R}^{m \times n}$ is the matrix measurement and $\eta \in \mathbb{R}^m$ is the noise. So given a pre-trained generative model $G: z \to x$, where $z \in \mathbb{R}^k$ and $x \in \mathbb{R}^n$, CSGM [3] introduced the objective

$$\hat{z} = \underset{z \in \mathbb{R}^k}{\arg \min} \|AG(z) - y\|^2 + \gamma \cdot \|z\|^2, \tag{1}$$

where both $\|\cdot\|$ are the 2-norm. Note that the network G was trained with similar samples than x^* , thus the intuition is to find \hat{z} such that the synthetic image $\hat{x} = G(\hat{z})$ is close to x^* .

Generative flows [6] have a particular advantage among generative models. Because they are invertible, they can perform the re-generation of any image—there exists a latent variable for any image x^* in an inverse problem, and is unique. Initially, generative flows were trained to solve a unique inverse problem [1]. Then, GlowIP [2] explored the use of a pre-trained generative flow to solve many inverse problems such as compressed sensing, denoising and inpainting.

As authors said in [3, 2], the intuition behind the regularization term $\|z\|^2$ (see Equation 1) is to encourage high likelihood latent variables because the generative model G is typically trained with the latent distribution $\mathcal{N}(\mathbf{0},\mathbf{I})$. However, a high log-likelihood in the latent representation may generate a low likelihood sample x. Indeed, the sample $x_0 = G(\mathbf{0})$ is a blurry and unlikely image in a generative flow (see Appendix C). Our hypothesis is that z must produce realistic samples instead. We therefore explore pre-trained generative flows as a general purpose solution for inverse problems by generating high likelihood reconstructions. We evaluate our method for image denoising, image deblurring, image inpainting and image colorization.

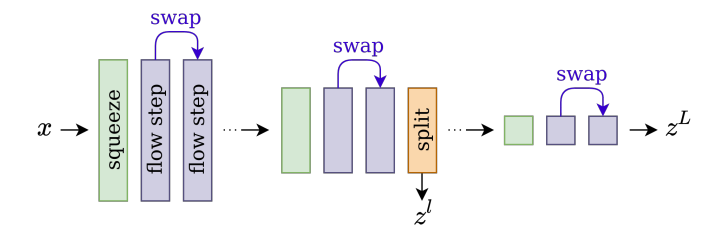


Figure 1: Our generative flow architecture. Each *flow step* is composed by an activation normalization [11] followed of a coupling layer. In addition, *swap* operations exchange the two partitions of hidden feature maps in intermediate coupling layers. We split low-scale latent variables in two chunks, and force one half (z^l) to follow p_Z . The other half continues its path until obtain a latent variable z^L of 1×1 scale

2 Background

Generative flows can be trained by the maximum likelihood using the change of variable formula

$$\log(p_X(x)) = \log(p_Z(z)) + \log(|\det \mathbf{J}_F(x)|), \tag{2}$$

where $F: x \to z$ is a bijection that maps from a sample $x \sim p_X$ to the latent variable $z \sim p_Z$, and $\mathbf{J}_F(x) = \frac{\partial F(x)}{\partial x}$ is the Jacobian of F evaluated at x. And F must be a transformation such that its Jacobian determinant is computationally tractable [6].

Recently, the Glow architecture [11] has been used as a pre-trained generative flow for inverse problems [2]. Glow introduces invertible 1x1 convolutions to learn permutations between channels, and re-scale the feature maps with squeeze layers [7]. Due to a squeeze layer should produce the same number of elements for a given input, the squeeze layer increments the number of channels that will be permuted by invertible 1x1 convolutions. This process increases the dimension of the invertible 1×1 convolution and consequently the computation cost of its Jacobian determinant in inference and its inverse in generation [11].

3 Method

3.1 1x1 Coupling layers

In order to save computational time during inference and generation, we perform a generative flow without invertible 1×1 convolutions. Inspired on [6], we perform swap operations that exchanges partitions in intermediate coupling layers (see Figure 1). Thus, every element of a given input h is modified in two coupling layers. To introduce permutation, our architecture encodes 1×1 hidden feature maps which are permuted by 1×1 convolutions in the next coupling layers. These convolutions do not require the computation of its Jacobian in inference or its inverse in the generation of samples. Additionally, based on [7], we force a half of low-scale feature maps z^l (see Figure 1) to follow the latent distribution. See the appendix for more information about the architecture.

3.2 Objective function

Let assume that we aim to recover $x^* \in \mathbb{R}^n$ from possible-noisy linear measurements $y = Ax^* + \eta$, where $A \in \mathbb{R}^{m \times n}$ and $\eta \in R^m$. Given a pre-trained generative flow $F_{\phi}: x \to z$ (parametrized by ϕ), where $x, z \in \mathbb{R}^n$, we may rewrite Equation 2 as

$$\log(p_{\phi}(x)) = \log(p_{Z}(z)) - \log(|\det \mathbf{J}_{F_{\phi}^{-1}}(z)|), \tag{3}$$

where $\log(p_{\phi}(x))$ is the log-likelikehood and $\mathbf{J}_{F_{\phi}^{-1}}(z) = \frac{\partial F_{\phi}^{-1}(z)}{\partial z}$ is the Jacobian of F_{ϕ}^{-1} evaluated at z. Note that the maximization of $\log(p_{Z}(z))$ is equivalent to the minimization of $\|z\|^{2}$, however it

Table 1: We compare our method with other objective functions and other types of initialization. The quality of reconstruction is measured using the PSNR and SSIM. The results is the average over 192 images.

Method	Denoising		Deblurring		Inpainting		Colorization	
	PSNR	SSIM	PSNR	SSIM	PSNR	SSIM	PSNR	SSIM
CSGM [3]	37.41	0.897	37.17	0.883	36.39	0.839	34.71	0.897
GlowIP [2]	37.21	0.894	35.82	0.867	37.81	0.903	35.79	0.937
BM3D [5]	37.65	0.905	_	_	_	_	_	_
Ours	37.72	0.918	39.72	0.963	37.97	0.913	35.72	0.940

does not ensure the maximization of the log-likelihood $\log(p_{\phi}(x))$ —we must maximize the Jacobian term as well. In contrast, the maximization of the right-hand side in Equation 3 directly ensures the generation of high log-likelihood samples x, which is what we pretend. Therefore, our objective function to find the latent variable that recovers x^* from y is

$$\hat{z} = \arg\min_{z \in \mathbb{R}^k} \left\{ \|AG(z) - y\|_1 + \alpha \cdot \left[\log(|\det \mathbf{J}_{F_{\phi}^{-1}}(z)|) - \log(p_Z(z)) \right] \right\},\tag{4}$$

where $\alpha>0$ is an hyperparameter, and we initialize the latent variable at $z_0 \sim \mathcal{N}(\mathbf{0}, \sigma^2 \mathbf{I})$. Furthermore, we find empirically that our regularization term $\log(|\det \mathbf{J}_{F_\phi^{-1}}(z)|) - \log(p_Z(z))$ performs better with the 1-norm than the 2-norm. The purpose of introducing the negative log-likelihood term into the main objective is to generate realistic images in the reconstruction process of inverse problems.

4 Results

We train a generative flow with the training samples of the CelebA dataset [12]. Once the network is fixed, we optimize Equation 4 and initialize with $\sigma=0.1$. To compare with other methods such as CSGM [3] and GlowIP [2], we perform their initialization and objective function in the same pre-trained generative flow. Note that CSGM and GlowIP perform the same objective function (Equation 1), the unique difference is the initialization: random initialization for CSGM and zero initialization for GlowIP. We therefore prove many values for their penalization hyperparameter γ because it improves their performance in some inverse problems. Additionally, in image denoising, we compare with BM3D [5]. Finally, we use the PSNR and SSIM metrics to measure the quality of reconstruction on each inverse problem.

Denoising For image denoising we use a noise level of $\sqrt{\mathbb{E}[\|\eta\|^2]}=0.1$. Figure 2 shows that CSGM ($\gamma=0.1$) smooths the noisy image but can not remove all distortions. These distortions are slightly more visible in GlowIP ($\gamma=0.1$) than CSGM. Surprisingly, our method outperforms BM3D in the PSNR and SSIM metrics as you can see in Table 1. Indeed, our reconstructions look sharper and more realistic than those from BM3D (see Figure 2). Nonetheless, our method eliminates some details from the background. In this case, we set $\alpha=0.05$ in Equation 4.

Deblurring We create synthetic blurry images by applying an average pooling in the target image x^* , and use it as the measurements y. There is no significant difference between CSGM ($\gamma=0.01$) and GlowIP ($\gamma=0$) in image deblurring (see Figure 3). Both produce visual artifacts that are exacerbated if we increase their penalization term—CSGM and GlowIP mitigate visual artifacts with $\gamma=0.01$ and $\gamma=0$ respectively. As you can see in Table 1, our method outperforms GlowIP and CSGM in the PSNR and SSIM metrics. Moreover, our results look more sharp and close to the original image. Our hyperparameter in this case is $\alpha=0.02$.

Inpainting For inpainting, we mask a square in the center of the target image and fill it with zeros. We obtain the best performance in CSGM for $\gamma = 0.01$. But even so, CSGM produces many visual artifacts. In contrast, GlowIP ($\gamma = 0$) produces a realistic reconstruction of the square of zeros with

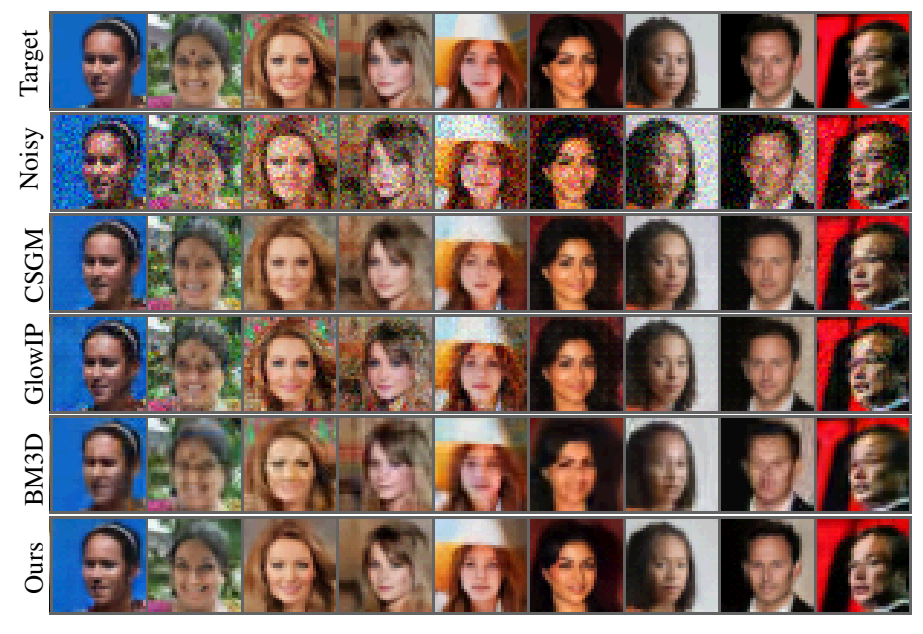


Figure 2: Image Denoising on CelebA images. We use a noise level of $\sqrt{\mathbb{E}[\|\eta\|^2]} = 0.1$.

few visual artifacts. As you can see in Table 1, our method slightly outperforms GlowIP, however our visual results look similar to those from GlowIP (see Figure 4). Apparently, the log-likelihood term does not significantly improve the performance. We obtain our best performance for $\alpha=0.002$.

Colorization In the case of the colorization problem, we average the three channels of the target image. CSGM ($\gamma=0.01$) generates over-saturated images that have different tones than the original image. Instead, GlowIP ($\gamma=0$) produces washed-out images, and similar to image deblurring, its regularization term does not improve its performance. Our method performs the colorization problem, however our results are similar to those from GlowIP. In this case, the log-likelihood term does not improve the performance in colorization. Table 1 shows our results for $\alpha=0.02$.

Our results show that Equation 1 produces some blur and visual artifacts in many inverse problems such as denoising and deblurring. This results in unrealistic reconstructions for CSGM and GlowIP in image denoising and deblurring. Although the $z_0 \sim \mathcal{N}(\mathbf{0}, \mathbf{I})$ initialization produces saturated images in image colorization, Table 1 shows better performance for $z_0 = \mathbf{0}$. Additionally, we find empirically that for CSGM is convenient to set $\gamma > 0$ on its Equation 1 to perform inverse problems. Instead, GlowIP produces its best results with $\gamma = 0$ in some inverse problems.

As you can see in Figure 6, high likelihood latent variables do not ensure realistic samples. Both CSGM and GlowIP have problems in image denoising and image deblurring. Additionally, in the case of inpainting, all methods (including ours) can not perform the reconstruction of non-frontal images. Maybe, a deeper generative flow could perform realistic reconstructions—our shallow generative flow use only 14 coupling layers in total. An analysis of continuous normalizing flows [4] as a pre-trained model is beyond the scope of this work.

5 Discussion

We demonstrate that the minimization of the negative log-likelihood as a regularization term improves the performance at denoising, deblurring and inpainting in low-resolution images. Indeed, our reconstructions are the sharpest and closest to the original image. Furthermore, we introduce 1×1 coupling layers to save computational time in the generation process. Our objective function ensures the generation of high likelihood samples which results in sharp reconstructions in inverse problems. It suggests that generative flows can be a general purpose solution for inverse problems with our method. Note that we use the same network for each inverse problem, we do not need to re-train a new network. A future direction is to evaluate our method for high-resolution images.

References

- [1] Lynton Ardizzone, Jakob Kruse, Carsten Rother, and Ullrich Köthe. Analyzing inverse problems with invertible neural networks. In *International Conference on Learning Representations*, 2019. URL https://openreview.net/forum?id=rJed6j0cKX.
- [2] Muhammad Asim, Max Daniels, Oscar Leong, Ali Ahmed, and Paul Hand. Invertible generative models for inverse problems: mitigating representation error and dataset bias. In Hal Daumé III and Aarti Singh, editors, *Proceedings of the 37th International Conference on Machine Learning*, volume 119 of *Proceedings of Machine Learning Research*, pages 399–409. PMLR, 13–18 Jul 2020. URL http://proceedings.mlr.press/v119/asim20a.html.
- [3] Ashish Bora, Ajil Jalal, Eric Price, and Alexandros G Dimakis. Compressed sensing using generative models. In *International Conference on Machine Learning*, pages 537–546. PMLR, 2017.
- [4] Ricky T. Q. Chen, Yulia Rubanova, Jesse Bettencourt, and David K Duvenaud. Neural ordinary differential equations. In S. Bengio, H. Wallach, H. Larochelle, K. Grauman, N. Cesa-Bianchi, and R. Garnett, editors, *Advances in Neural Information Processing Systems*, volume 31. Curran Associates, Inc., 2018. URL https://proceedings.neurips.cc/paper/2018/file/69386f6bb1dfed68692a24c8686939b9-Paper.pdf.
- [5] Kostadin Dabov, Alessandro Foi, Vladimir Katkovnik, and Karen Egiazarian. Image denoising by sparse 3-d transform-domain collaborative filtering. *IEEE Transactions on image processing*, 16(8):2080–2095, 2007.
- [6] Laurent Dinh, David Krueger, and Yoshua Bengio. Nice: Non-linear independent components estimation. *arXiv preprint arXiv:1410.8516*, 2014.
- [7] Laurent Dinh, Jascha Sohl-Dickstein, and Samy Bengio. Density estimation using real nvp. In *International Conference on Learning Representations 2017 (Conference Track)*, 2017. URL https://openreview.net/forum?id=HkpbnH91x.
- [8] Ian Goodfellow, Jean Pouget-Abadie, Mehdi Mirza, Bing Xu, David Warde-Farley, Sherjil Ozair, Aaron Courville, and Yoshua Bengio. Generative adversarial nets. In Z. Ghahramani, M. Welling, C. Cortes, N. Lawrence, and K. Q. Weinberger, editors, Advances in Neural Information Processing Systems, volume 27. Curran Associates, Inc., 2014. URL https://proceedings.neurips.cc/paper/2014/file/5ca3e9b122f61f8f06494c97b1afccf3-Paper.pdf.
- [9] Diederik P. Kingma and Jimmy Ba. Adam: A method for stochastic optimization. In Yoshua Bengio and Yann LeCun, editors, 3rd International Conference on Learning Representations, ICLR 2015, San Diego, CA, USA, May 7-9, 2015, Conference Track Proceedings, 2015. URL http://arxiv.org/abs/1412.6980.
- [10] Diederik P. Kingma and Max Welling. Auto-Encoding Variational Bayes. In 2nd International Conference on Learning Representations, ICLR 2014, Banff, AB, Canada, April 14-16, 2014, Conference Track Proceedings, 2014.
- [11] Durk P Kingma and Prafulla Dhariwal. Glow: Generative flow with invertible 1x1 convolutions. In S. Bengio, H. Wallach, H. Larochelle, K. Grauman, N. Cesa-Bianchi, and R. Garnett, editors, *Advances in Neural Information Processing Systems*, volume 31. Curran Associates, Inc., 2018. URL https://proceedings.neurips.cc/paper/2018/file/d139db6a236200b21cc7f752979132d0-Paper.pdf.
- [12] Ziwei Liu, Ping Luo, Xiaogang Wang, and Xiaoou Tang. Deep learning face attributes in the wild. In *Proceedings of the IEEE international conference on computer vision*, pages 3730–3738, 2015.

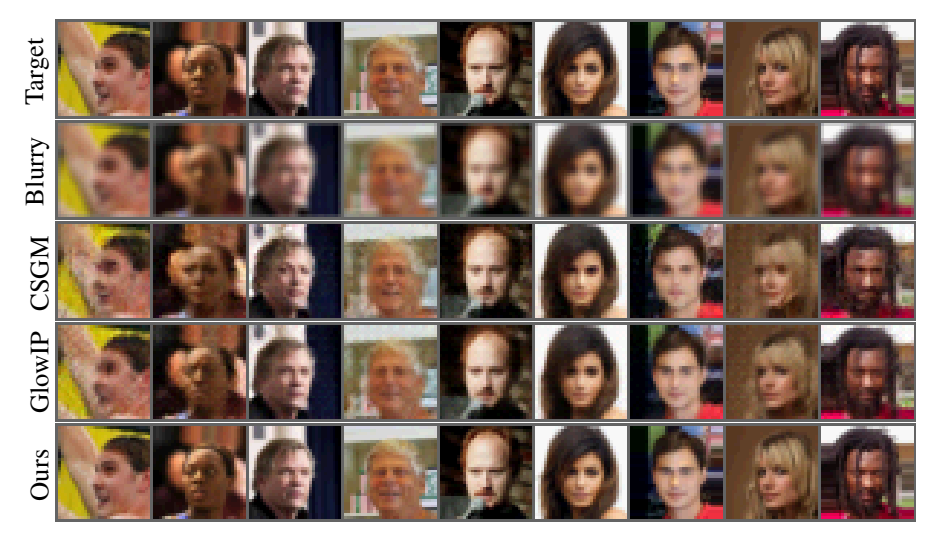


Figure 3: Image deblurring on CelebA images. We create synthetic blurry images by applying a 3×3 average pooling with stride 1 on the targets.

A Generative flow architecture

Coupling layers in our model perform the following operations

$$h_k, h_p = \text{swap}(\text{split}(h))$$
 (5)

$$s, t = NN(h_k) \tag{6}$$

$$s = \operatorname{sigmoid}(s+2) \tag{7}$$

$$h_c = h_p \odot s + t \tag{8}$$

$$r = \operatorname{concat}(\operatorname{swap}(h_k, h_c)), \tag{9}$$

where h is the input tensor and r is the output. Note that if we apply a swap operation in Equation 5, then we should apply another in Equation 9 to hold the order of the elements. NN respectively applies 1×1 , 2×2 and 3×3 convolutions without padding for feature maps with scales 1×1 , 2×2 and 3×3 . Hence, each 1×1 convolution permutes the elements of h_k because the scale of h_k is 1×1 . Furthermore, Inspired on [11], we apply activation normalization before the pair of coupling layers. Finally, we use 512 hidden channels in the network NN.

B Training configuration

We train our generative flow and solve inverse problems using Adam [9]. CelebA images are resized to 32×32 resolution and we use the test set to evaluate each method. Additionally, our generative flow uses K=2 and L=5, and duplicate K for scales 2×2 and 1×1 —we use 14 coupling layers in total. We train the generative flow with a batch size of 32 and stop the training process after 100 epochs. Then, we solve each inverse problem with 1500 iterations and a learning rate of 0.005. All experiments were made in a GeForce GTX 750 Ti.

C Additional experiments

Due to our generative flows was trained with a latent distribution $\mathcal{N}(\mathbf{0},\mathbf{I})$, one must use this distribution to sample realistic images. Hence, we conduct an experiment for different values of the standard deviation of the latent distribution. Given a latent variables $z \sim \mathcal{N}(\mathbf{0}, \sigma^2\mathbf{I})$ in a pre-trained generative flow $F_{\phi}: x \to z$ (parametrized by ϕ), we sample for many values of σ as you can see in Figure 6. Our experiments show that if we initialize at $z_0 = 0$, the sample $F^{-1}(z_0) = x_0$ is a blurry and unrealistic image. As we increase the standard deviation in the latent variables, we generate high

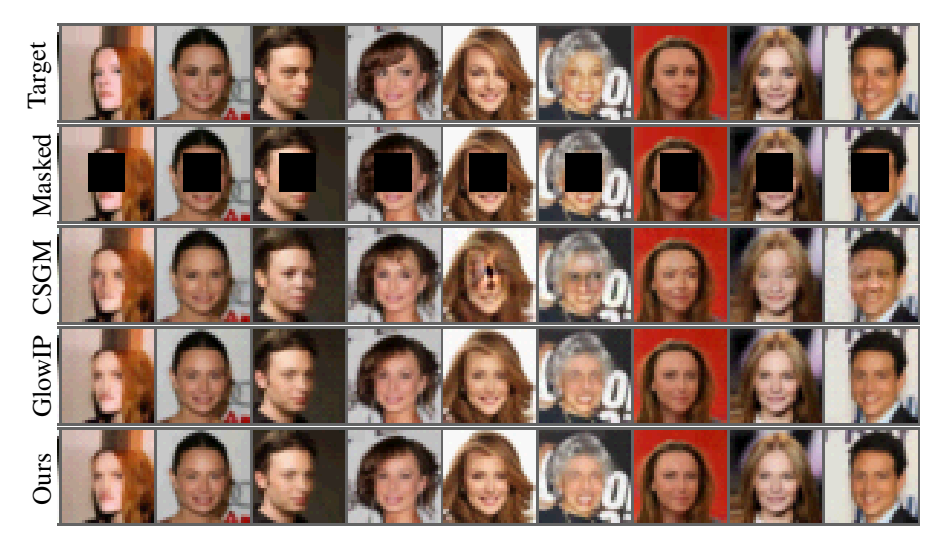


Figure 4: Image Inpainting on CelebA images. We crop a region of images to create the masked images.

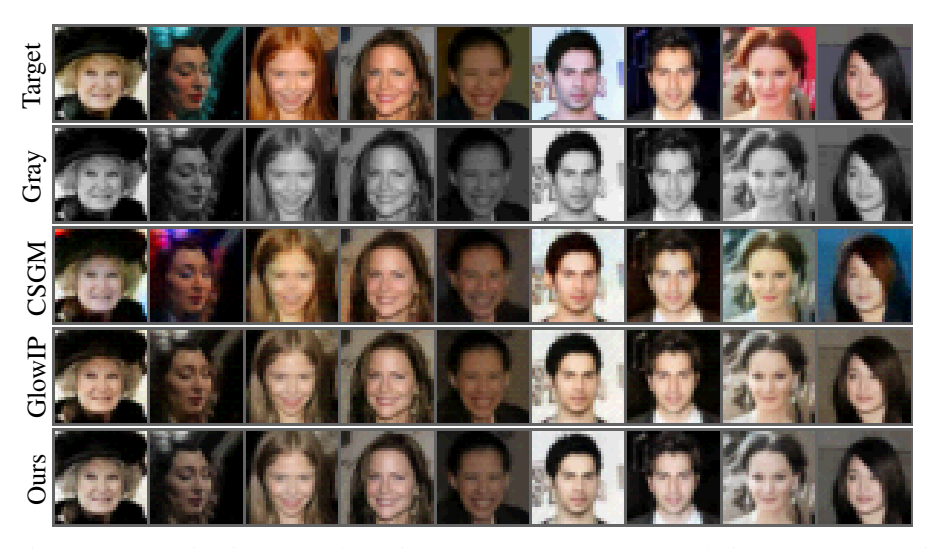


Figure 5: Image Colorization on CelebA images. We create gray scale images by averaging the channels of the target images.

likelihood samples, however we also introduce visual artifacts. Figure 6 shows that latent variables with a σ in [0.8, 1.2] produces the most realistic samples. Additionally, we also show the visual results for image deblurring, image colorization and image inpainting. Figures 3, 4 and 5 show visual results for 9 samples. For these inverse problems, we compare with CSGM [3] and GlowIP [2].



Figure 6: Samples from our pre-trained generative flow. We generate images from an isotropic Gaussian distribution $\mathcal{N}(\mathbf{0}, \sigma^2 \mathbf{I})$. Each row represent a batch of 16 samples by setting a different value for σ . Note that $\sigma=0$ represents $z=\mathbf{0}$.